IPC

**Indonesian Physics Communication**

Department of Physics, Universitas Riau, Pekanbaru, Indonesia
p-ISSN 1412-2960 | e-ISSN 2579-521X

Vol. 22 | No. 3
November 2025

Web: https://kfi.ejournal.unri.ac.id
E-mail: kfi@ejournal.unri.ac.id

# Preparation and characterization of α-$Fe_2O_3$/$TiO_2$ nanocomposite derived from Logas natural sand as photocatalyst for degradation of methylene blue

**Muhammad Deri Noferdi, Erwin Amiruddin***
Department of Physics, Universitas Riau, Pekanbaru 28293, Indonesia

Corresponding author: erwin.amiruddin@lecturer.unri.ac.id

## ABSTRACT

In this study, we prepared iron oxide/titanium dioxide (α-$Fe_2O_3$/$TiO_2$) nanocomposites based on Logas natural sand using a ball milling method. The effect of milling time on the magnetic properties and chemical composition of the nanocomposites was studied using a vibrating sample magnetometer (VSM) and X-ray fluorescence (XRF), respectively. The magnetization versus external magnetic field measurements used for all samples indicated ferromagnetic behavior, characterized by low coercivity values ranging from 360.10 Oe to 86.50 Oe for milling times of 50 to 200 hours, respectively. The XRF results indicated that several other elements, such as silicon, aluminum, and others, were detected, indicating that the milled nanocomposites (α-$Fe_2O_3$/$TiO_2$) were impure. The methylene blue degradation efficiency of α-$Fe_2O_3$/$TiO_2$ nanocomposites increases with increasing milling time.

**Keywords:** Ball milling; iron oxide/titanium dioxide; Logas natural sand; methylene blue; nanocomposite

Received 03-08-2025 | Revised 24-08-2025 | Accepted 10-11-2025 | Published 15-11-2025

## INTRODUCTION

One of the most used synthetic dyes is methylene blue (MB), releasing methylene blue into the environment can cause various problems. MB is toxic, carcinogenic, and non-biodegradable, posing various environmental hazards to aquatic and terrestrial life. The dangers of MB can also harm human health in multiple ways, such as respiratory disorder, abdominal pain, blindness, and digestive issues [1, 2]. Because of this, various treatment methods have been used to remove MB from environment.

Advanced oxidation processes (AOP) is one of the methods to remove methylene blue from environment, it is a promising, efficient, and environmentally friendly method [3, 4]. Among various AOP methods, the photo-Fenton method has garnered widespread attention due to its high efficiency and environmental friendliness. This method uses ultraviolet (UV) radiation to enhance the production of hydroxyl radicals and improve the overall efficiency of the degradation process. In the photo-Fenton, UV irradiation significantly enhances pollutant degradation by regenerating $Fe^{2+}$ from $Fe^{3+}$, thereby sustaining the catalytic cycle and increasing hydroxyl radical production [5].

Iron oxides is one of the most used catalysts in photo-Fenton process. They have unique properties, apart from having a short energy band gap, this material is also magnetic, so it is easy to recycle. Iron oxides are divided into three main types, namely hematite (α-$Fe_2O_3$) which is most widely used as a photocatalyst, as well as maghemite (γ-$Fe_2O_3$) and magnetite ($Fe_3O_4$) which are applied in drug delivery, energy storage, and data storage [6].

Iron oxide α-$Fe_2O_3$ is a photocatalyst with good stability, low cost, and short band gap energy (2.1 eV) so it shows good visible light response. Iron oxide α-$Fe_2O_3$ has several disadvantages such as poor absorptivity and low electrical conductivity which cause high charge recombination resulting in low photoactivity [7, 8]. This weakness can be overcome by combining α-$Fe_2O_3$ with other iron oxides such as $TiO_2$, to obtain α-$Fe_2O_3$/$TiO_2$ nanocomposites. By combining α-

$Fe_2O_3$ with $TiO_2$, charge transfer is increased, and electron-hole recombination is suppressed, thereby enhancing the photocatalytic activity [9]. To obtain iron oxide α-$Fe_2O_3$ with controlled size, various methods have been developed such as hydrothermal, sol-gel, microwave, and ball milling. Ball milling is one of the best choices [10], because this method is simple, efficient, and cost-effective [11-13].

In recent years, research on α-$Fe_2O_3$/$TiO_2$ nanocomposite has been widely conducted. $TiO_2$/α-$Fe_2O_3$ composite derived from iron sand via mechanical ball milling method demonstrated high photodegradation activity (100%) against indigo carmine dye under UV irradiation [14]. Another research found using a simple co-precipitation method, $Fe_2O_3$@50% $TiO_2$ nanocomposites performed the best as a photocatalyst to degrade MB under visible light [15].

In this study, α-$Fe_2O_3$/$TiO_2$ nanocomposite were derived from natural sand of Logas village. Natural sands were prepared using 4-stage ball milling method. The resulting product were analyzed using X-ray diffraction (XRD), X-ray fluorescence (XRF) spectroscopy, and vibrating sample magnetometer (VSM) to investigate the structural, elemental composition and magnetic properties of α-$Fe_2O_3$/$TiO_2$ nanocomposite. Using photo-Fenton method, methylene blue degradation efficiency of samples was investigated.

## EXPERIMENTAL PROCEDURE

### Material and Chemical

The material used to prepare α-$Fe_2O_3$/$TiO_2$ nanocomposites was natural sand from Logas Village, Kuansing District, Riau Province. The chemical used included methylene blue ($C_{16}H_{18}ClN_3S$), hydrogen peroxide ($H_2O_2$) 30%, and aqua DM.

### Preparation of α-$Fe_2O_3$/$TiO_2$ Photocatalyst

Before the ball milling process began, natural sand was first processed using iron sand separator and NdFeB magnet to separate iron oxide and non-iron oxide particles from samples. The ball milling process conducted in four stages, each stage lasted for 50 hours. After each stage, iron oxide and non-iron oxide separated using NdFeB magnets. Four products from the ball milling process were then characterized using X-ray diffraction (XRD), X-ray fluorescence (XRF) spectroscopy, and vibrating sample magnetometer (VSM) to analyze the structural properties, chemical composition, and magnetic properties of samples.

### Methylene Blue Degradation

The methylene blue (MB) degradation experiment was performed in a black box, using a 250-watt mercury lamp as the light source. 1-gram of α-$Fe_2O_3$/$TiO_2$ catalyst was mixed with 100 ml MB (30 ppm) in each test. First, the solution was mixed with magnetic stirrer in the dark environment for 40 minutes to reach an adsorption–desorption equilibrium. After 40 minutes, the light source was turned on and then 5 ml hydrogen peroxide were added to solution, at interval of 0, 10, 20, 40, 60, 80, 100, and 120 minutes, 6 ml sample were collected from solution. Samples were centrifuged for 5 minutes at 3000 rpm, this process repeated until the catalyst precipitate removed. Absorbance was measured using UV–vis spectrophotometer at a wavelength of 660 nm. The percentage of MB degradation can be calculated using following Equation (1):

$$\text{Degradation MB (\%)} = \frac{C_0 + C_t}{C_0} \times 100\% \qquad (1)$$

where, $C_0$ is concentration of initial MB and $C_t$ is concentration of MB after irradiation.

## RESULTS AND DISCUSSION

### Structural Analysis

The XRD pattern of α-$Fe_2O_3$/$TiO_2$ nanocomposite from 4 stage milling process

and pure $Fe_2O_3$ are shown in Figure 1. The prominent peaks of α-$Fe_2O_3$/$TiO_2$ nanocomposites of 50 hours milling time were detected at about 2θ = 23.93°, 32.79°, 35.38°, 40.51°, 48.94°, 53.45°, 56.75°, 61.81°, 63.49°, and 70.86°, which are associated with the (102), (104), (110), (113), (024), (116), (122), (214), (300), and (119) of crystal planes hexagonal hematite (JCPDS No. 89-8103). The presence of two additional peaks also detected at 2θ = 26.68° and 38.69°, corresponding to the diffraction planes (111) and (004). The peak (111) was observed in BM 1, BM 2, and BM 3 products, the presence of a peak at (111) indicates that silicon was present in the samples. The peak at (004) indicated the present of $TiO_2$ anatase phase within the samples, this means that the 4-stage ball milling process has successfully produced α-$Fe_2O_3$/$TiO_2$ nanocomposite. Other than these two additional peaks, other observable difference XRD pattern between BM products and pure α-$Fe_2O_3$ also found. There was a decrease in the intensity of the main peaks and slight shift of angles of hematite in XRD pattern of ball milling products due to cooperation of α-$Fe_2O_3$ and $TiO_2$.

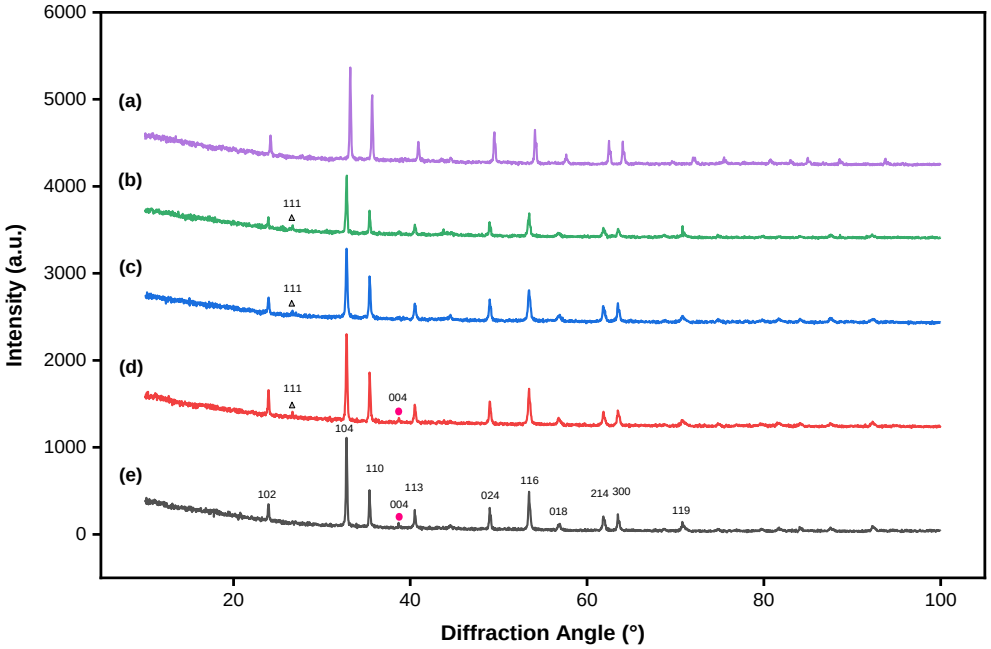


**Figure 1.** XRD patterns of: (a) pure $Fe_2O_3$ and α-$Fe_2O_3$/$TiO_2$ nanocomposites for different milling time (b) 50 hours (c) 100 hours (d) 150 hours (e) 200 hours.

The average crystallite size could be calculated using Scherrer's equation based on the determined lattice parameters as follows [16]:

$$D = k\lambda/\beta cos\theta \quad (2)$$

where D is the average crystallite size, k is Scherrer's constant, λ is the X-ray wavelength, β is the full-width half maximum (FWHM) of the XRD peaks, and θ is the peak angle [8]. The calculations using Scherrer's equation show that the average crystallite size of α-$Fe_2O_3$/$TiO_2$ nanocomposites decreased monotonically from 57.09 nm to 51.14 nm as shown in Figure 2.

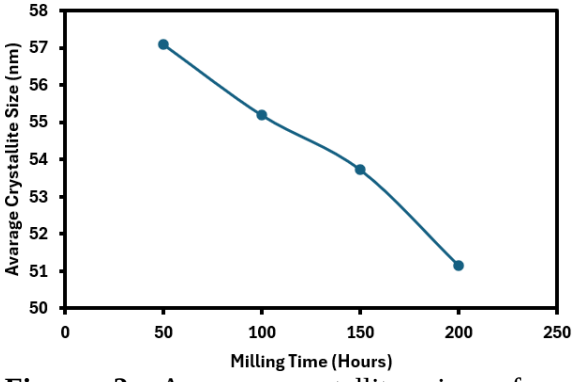


**Figure 2.** Average crystallite size of α-$Fe_2O_3$/$TiO_2$ nanocomposites based on all prominent peak.

## Elemental Composition

The chemical composition of ball milling products with different variations of milling time, analyzed using X-ray fluorescence (XRF) Spectroscopy. The percentage of α-$Fe_2O_3$, $TiO_2$, and $SiO_2$ are presented in Figure 3.

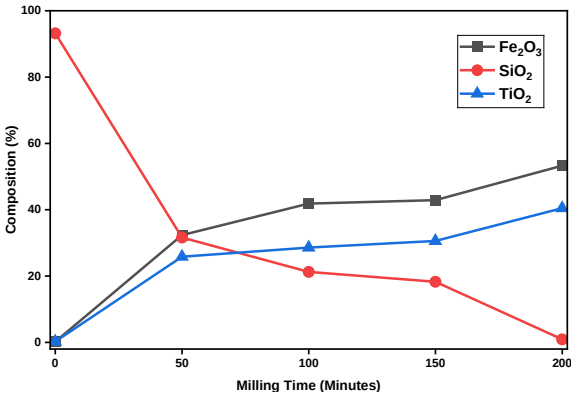


**Figure 3.** The percentage of (a) α-$Fe_2O_3$, (b) $TiO_2$, and (c) $SiO_2$ for milling products with time variations of 50, 100, 150, and 200 hours.

The percentage of α-$Fe_2O_3$ and $TiO_2$ increases from 0.166 to 53.274% and 0.225 to 40.464% respectively, while SiO2 decreases from 93.209% to 0.9% along with the increase in milling time used, with 200 hours of milling time having the highest percentage of α-$Fe_2O_3$ and $TiO_2$, also with the lowest impurity.

This shows that the 4-stage ball milling process for 200 hours and separation using NdFeB magnets after each stage successfully eliminated most of the silicon from the sample, although there were still impurities in the form of silicon and other oxides in the sample in low quantities.

## Magnetic Properties

The hysteresis loop measurement of α-$Fe_2O_3$/$TiO_2$ nanocomposites was carried out using vibration sample magnetometer (VSM), the applied magnetic field used ranged from -20.000 Oe to +20.000 Oe, as can be seen in Figure 4.

From Figure 4, it is clear that all samples show ferromagnetic behavior, the samples have low coercivity and remanence values. Table 1 shows the magnetic parameters of α-$Fe_2O_3$/$TiO_2$ nanocomposites with different milling times, which include saturation magnetization ($M_s$), remanent magnetization ($M_r$), and coercivity ($H_c$). The Ms value increases as the milling time increases, which is likely due to higher proportion of α-$Fe_2O_3$ in nanocomposite. This leads to increase in magnetic moment per unit mass, resulting in higher magnetization value. This result is in agreement with previous studies [17].

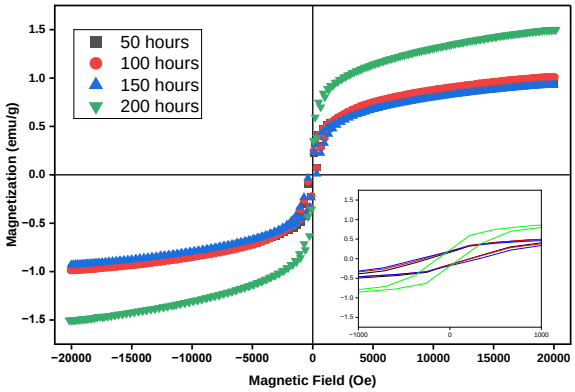


**Figure 4.** Hysteresis loop of α-$Fe_2O_3$/$TiO_2$ nanocomposite with variations of milling time, with an inset showing the enlarged loop of samples.

The coercivity value of α-$Fe_2O_3$/$TiO_2$ for milling time of 50 h is about 349.2 Oe, then increase to 357.94 Oe and 360.08 Oe for 100 h and 150 h respectively. The coercivity value experienced a significant decrease to 88.5 Oe at 200 hours of milling time. This decrease in coercivity value suggests that the material becomes more superparamagnetic.

**Table 1.** Magnetic parameters of α-$Fe_2O_3$/$TiO_2$ nanocomposites.

| Milling time (hours) | $M_s$ (emu/g) | $M_r$ (emu/g) | $H_c$ (Oe) |
|---|---|---|---|
| 50 | 0.954 | 0.157 | 349.20 |
| 100 | 0.998 | 0.175 | 357.94 |
| 150 | 1.299 | 0.182 | 360.08 |
| 200 | 1.508 | 0.201 | 88.50 |

## Photocatalytic Activity of α-$Fe_2O_3$/$TiO_2$

The photocatalytic activity of α-$Fe_2O_3$/$TiO_2$ nanocomposite using photo-Fenton method

were investigated. Figure 5 shows the degradation efficiency of ball milling products as function of irradiation time.

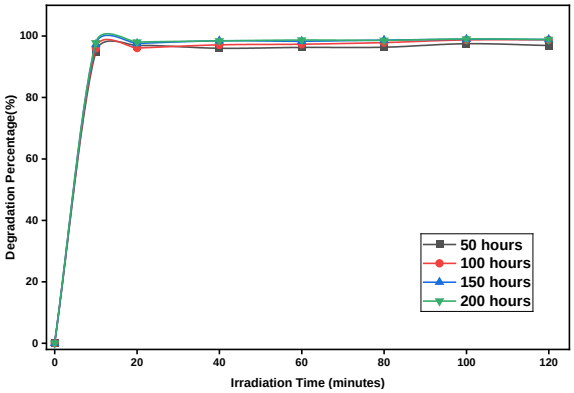


**Figure 5.** Methylene blue degradation efficiency.

As observed from Figure 5, within just 10 minutes of irradiation time all α-$Fe_2O_3$/$TiO_2$ nanocomposite catalysts show degradation rate of over 94 %. Similar results also found by previous studies, they explained that the high degradation rate at first minutes happen because of the high initial concentration of MB [18]. The strong driving force caused by the high concentration difference promotes the adsorption of MB on the material, thereby accelerating the subsequent photodegradation reaction rate [18].

All four catalysts exhibited excellent photocatalytic performance. The maximum degradation rate of α-$Fe_2O_3$/$TiO_2$ nanocomposites prepared with 50 hours milling is 97.46 %, and then increase to 97.73%, 98.92%, and 99.00% with increasing milling time of 100, 150, and 200 hours, respectively. The increases of degradation rate with increasing milling time happen because of the decrease of crystallite size, resulting in a higher specific surface area. This provides more active sites for photocatalyst to interact with MB, generating more reactive radicals species.

## CONCLUSION

In this study, iron oxide (α-$Fe_2O_3$)/$TiO_2$ nanocomposites were successfully prepared by ball milling method. The results of VSM measurements showed that the magnetic properties of iron oxide (α-$Fe_2O_3$)/$TiO_2$ nanocomposites were affected by increasing milling time. Magnetization ($M_s$) and remanance magnetization ($M_r$) increased with increasing milling time, while the coercivity ($H_c$) of the sample increased with increasing milling time up to 100 hours and decreased rapidly after 150 hours. Iron oxide (α-$Fe_2O_3$) and titanium dioxide ($TiO_2$) nanoparticles both increased and silicon oxide ($SiO_2$) and others decreased with increasing milling time. The maximum degradation rate of α-$Fe_2O_3$/$TiO_2$ nanocomposites prepared with 50 hours milling is 97.46 %, and then increase to 97.73%, 98.92%, and 99.00% with increasing milling time of 100, 150, and 200 hours, respectively.

## REFERENCES


1. Al-Tohamy, R., Ali, S. S., Li, F., Okasha, K. M., Mahmoud, Y. A. G., Elsamahy, T., ... & Sun, J. (2022). A critical review on the treatment of dye-containing wastewater: Ecotoxicological and health concerns of textile dyes and possible remediation approaches for environmental safety. *Ecotoxicology and Environmental Safety*, **231**, 113160.
2. Khan, I., Saeed, K., Zekker, I., Zhang, B., Hendi, A. H., Ahmad, A., Ahmad, S., Zada, N., Ahmad, H., Shah, L. A., Shah, T., & Khan, I. (2022). Review on methylene blue: its properties, uses, toxicity and photodegradation. *Water*, **14**(2), 242.
3. Charitha, T., Leshan, U., Shanitha, M., Ramanee, W., Buddi, L., & Martin, B. (2021). Efficient photodegradation activity of α-$Fe_2O_3$/$Fe_2TiO_5$/$TiO_2$ and $Fe_2TiO_5$/$TiO_2$ nanocomposites synthesized from natural ilmenite. *Results in Materials*, **12**, 100219.
4. Hübner, U., Spahr, S., Lutze, H., Wieland, A., Rüting, S., Gernjak, W., & Wenk, J. (2024). Advanced oxidation processes for water and wastewater treatment–Guidance

for systematic future research. *Heliyon*, **10**(9).
5. Całus-Makowska, K., Dziubińska, J., Grosser, A., & Grobelak, A. (2025). Application of the Fenton and photo-Fenton processes in pharmaceutical removal: New perspectives in environmental protection. *Desalination and Water Treatment*, **321**, 100949.
6. Campos, E. A., Pinto, D. V. B. S., Oliveira, J. I. S. D., Mattos, E. D. C., & Dutra, R. D. C. L. (2015). Synthesis, characterization and applications of iron oxide nanoparticles-a short review. *Journal of Aerospace Technology and Management*, **7**(3), 267–276.
7. Lubis, S., Sheilatina, & Murisna. (2018). Synthesis, characterization and photocatalytic activity of α-Fe2O3/bentonite composite prepared by mechanical milling. *Journal of Physics: Conference Series*, **1116**(4), 042016).
8. AlSalka, Y., Granone, L. I., Ramadan, W., Hakki, A., Dillert, R., & Bahnemann, D. W. (2019). Iron-based photocatalytic and photoelectrocatalytic nano-structures: Facts, perspectives, and expectations. *Applied Catalysis B: Environmental*, **244**, 1065–1095.
9. Kouass, S., Dhaouadi, H., Othmani, A., & Touati, F. (2021). *Characterization, Photoelectric Properties, Electrochemical Performances and Photocatalytic Activity of the $Fe_2O_3/TiO_2$ Heteronanostructure*. Electrocatalysis and Electrocatalysts for a Cleaner Environment-Fundamentals and Applications.
10. Erwin, E. & Putra, S. U. (2018). Sifat Magnetik Dan Ukuran Partikel Magnetik Serta Komposisi Material Pasir Besi Pantai Kata Pariaman Sumatera Barat Di Sintesa Dengan Iron Sand Separator Dan Ball Milling. *Journal Online of Physics*, **3**(2), 11–14.
11. Sihombing, M. & Amiruddin, E. (2020). Sintesis Dan Karakterisasi Nanopartikel $Fe_2O_3$ Dari Pasir Alam Desa Logas Kabupaten Kuantan Singingi. *Komunikasi Fisika Indonesia*, **17**(2), 68–73.
12. Salomo, S., Erwin, A., Usman, M., Muhammad, H., Nita, Y., & Linda, W. (2020). Preparation of Iron Oxide Magnetic Nanoparticles Natural Sand of Rokan River Synthesis with Ball Milling. *Journal of Physics: Conference Series*, **1655**(1), 012018.
13. Amiruddin, E., Awaluddin, A., Rini, A. S., Umar, L., Rianna, M., Hadilala, T. P., & Putri, N. (2024). Magnetic and Optical Properties of α-$Fe_2O_3/TiO_2$ Nanocomposite Derived from Logas Natural Sand for Environmental Application. *Journal of Physics: Conference Series*, **2908**(1), 012003.
14. Lubis, S. & Maulana, I. (2018). Synthesis and characterization of $TiO_2$/α-$Fe_2O_3$ composite using hematite from iron sand for photodegradation removal of dye. *Jurnal Natural*, **18**(1), 38–43.
15. Mansour, H., Omri, K., Bargougui, R., & Ammar, S. (2020). Novel α-Fe2O3/TiO2 nanocomposites with enhanced photocatalytic activity. *Applied Physics A*, **126**(3), 151.
16. Cullity, B. D. (1986). *Elements of X-ray Diffraction*. Hsin Yueh.
17. Amiruddin, E., Hadianto, H., Riana, M., Sinuraya, S., Noverdi, M. D., & Fitri, A. S. (2021). Undoped and manganese doped iron oxide nanoparticles for environmental applications. *ARPN Journal of Engineering and Applied Sciences*, **16**(18).
18. Liu, L., Cui, Z., Feng, B., Sui, M., Huang, H., & Wu, Z. (2024). Synthesis of $Fe_2O_3/TiO_2$ Photocatalytic Composites for Methylene Blue Degradation as a Novel Strategy for High-Value Utilisation of Iron Scales. *Materials*, **17**(18), 4546.